mathematics

Article

Analytical Solutions of Partial Differential Equations Modeling the Mechanical Behavior of Non-Prismatic Slender Continua

Giovanni Migliaccio [1,2]

[1] Department of Civil, Construction-Architectural and Environmental Engineering, University of L'Aquila, 67100 L'Aquila, Italy; giovanni.migliaccio@univaq.it
[2] National Group for Mathematical-Physics (GNFM), 67100 L'Aquila, Italy

Abstract: Non-prismatic slender continua are the prototypical models of many structural elements used in engineering applications, such as wind turbine blades and towers. Unfortunately, closed-form expressions for stresses and strains in such continua are much more difficult to find than in prismatic ones, e.g., the de Saint-Venant's cylinder, for which some analytical solutions are known. Starting from a suitable mechanical model of a tapered slender continuum with one dimension much larger than the other tapered two, a variational principle is exploited to derive the field equations, i.e., the set of partial differential equations and boundary conditions that govern its state of stress and strain. The obtained equations can be solved in closed form only in a few cases. Paradigmatic examples in which analytical solutions are obtainable in terms of stresses, strains, or related mechanical quantities of interest in engineering applications are presented and discussed.

Keywords: tapered cylinder; non-prismatic beam; cross-sectional warping; strain flow

MSC: 35C05; 35A09; 35B30; 74G05; 74K10

check for updates

Citation: Migliaccio, G. Analytical Solutions of Partial Differential Equations Modeling the Mechanical Behavior of Non-Prismatic Slender Continua. *Mathematics* **2023**, *11*, 4723. https://doi.org/10.3390/math11234723

Academic Editor: Alberto Ferrero

Received: 31 October 2023
Revised: 18 November 2023
Accepted: 20 November 2023
Published: 22 November 2023

1. Introduction

Non-prismatic slender elements are widely employed in engineering applications for their structural efficiency compared to prismatic ones, but their peculiar shape makes it complex to predict their state of stress and strain via analytical methods. Examples are components of aircraft, wind turbines, and civil structures [1–5]. The prototypical model for elements of this kind is that of the non-prismatic slender elastic continuum, i.e., a three-dimensional elastic body with one dimension, say, the longitudinal one, much larger than the other two, which are variable along the longitudinal dimension.

Since the early 20th century, several models have been proposed for slender structural elements, e.g., the linear beam theory in classical treatises on the theory of elasticity [6–8]; Simo's geometrically exact approach [9], which can be seen as a generalization of Reissner's formulation [10,11] and a convenient parameterization of the Antman's extension [12] of the Kirchhoff–Love rod model; numerically oriented formulations, e.g., [13,14]; formulations based on the Cosserats (directed continuum) approach [15,16]; models based on asymptotic methods, such as the one proposed by Berdichevsky [17] and subsequently exploited by Hodges et al. [18,19]; and other refined beam models, e.g., [20–22], improving classical theories via shear correction factors or specific warping functions.

Moreover, particular attention has been devoted to models that explicitly account for the influence of peculiar geometric features. Among them, we recall investigations concerning the cross-sectional pre-twist [23–28], aimed at analytically studying the effects on stresses and strains induced by variations in cross-section orientation (pre-twist), and studies regarding the influence of variable cross-section dimensions (taper), for which more sophisticated models are needed [5,29–31]. The influence of taper, in particular, has been studied by several scholars in different fields [32–38]. Focusing the attention on the effects of taper on stresses and strains, most works assumed Navier's formula [39] to hold for the cross-sectional normal stresses and derived the relevant shear stresses via the static equilibrium of the beam in its reference undeformed configuration, following Jourawksi's method [40]. In the field of civil engineering, we recall the early work of Bleich [41] on variable depth beams, as well as the studies of Paglietti and Carta [5] and Balduzzi et al. [42]. In the aerospace sector, Atkin [1] addressed the study of stresses and strains in typical aircraft elements with tapered cross-sections, Pugsley and Weatherhead [43] investigated the failures of tail-plane spars in highly tapered regions, and Saksena [44] proposed formulas for shear stresses in some tapered components. For wind engineering applications, Bertolini et al. [38] and Migliaccio et al. [4,31] studied the stress distributions in the cross-sections of wind turbine blades and towers. However, despite the progress made over the years and the numerous works in the literature, the analytical determination of cross-sectional stresses and strains, both in- and out-of-plane, in non-prismatic slender elements, still deserve investigation. Notwithstanding the slender shape of such elements, an analytical prediction of the effects of taper cannot be based on the results valid for the de Saint-Venant's cylinder [7,8], but a tailored model is needed because of the non-trivial stress and strain fields (produced by taper) that are absent in prismatic cases and that are unpredictable via prismatic beam theories [5,35,45,46].

This work addresses the physical–mathematical modeling and the analytical prediction of the state of stress and strain in non-prismatic slender bodies susceptible to large deflections. A variational principle is exploited to derive the field equations that govern the mechanical behavior of such bodies. They include a new set of partial differential equations (PDEs) with Neumann-type boundary conditions that explicitly account for the influence of taper on the in- and out-of-plane cross-sectional stresses and strains, represent a generalization of the PDEs that governs the state of stress and strain in the de Saint-Venant's cylinder, and reduce exactly to these latter in the absence of taper (prismatic case). Partial differential equations, with appropriate boundary conditions, represent the prototypical mathematical model of many physical problems [7,8,47–49]. Unfortunately, they cannot be solved in closed form in general. This is also the case of the PDE problem formulated in this work, which can always be solved numerically, but admits closed-form solutions only in a few cases. Specifically, as is demonstrated in the paper, we can obtain closed-form expressions for stress and strain fields in non-prismatic slender elements with particular cross-sectional shapes, as well as analytical solutions for other mechanical quantities of interest in applications (e.g., cross-sectional strain flow) for elements with generic cross-sectional shapes. The reported analytical solutions allow, in particular, the analytical demonstration of the inadequacy of stepped beam approaches when dealing with stress predictions in tapered beams and provide an insight into the physical problem that is not achievable via purely numerical investigations. For more clarity, we specify that in the present work the term solution refers to classical solutions (not weak solutions) of the PDE problem, while analytical solution refers to a solution given in terms of closed-form expressions or formulas (i.e., not numerical).

The paper is organized as follows. The general physical–mathematical model and the relevant PDEs that describe the mechanical behavior of the considered elastic body are introduced in Section 2. Analytical solutions for tapered beams with circular cross-sections are reported in Section 3. Closed-form solutions valid for generic cross-sectional shapes in terms of cross-sectional strain flow are proposed in Section 4. Finally, conclusions are drawn and possible prospects are illustrated in Section 5.

2. Mechanical Model

Mechanical modeling of deformable bodies requires three main ingredients: (1) a description of the state of relative motion between the body points, which involves defining quantities called strain measures; (2) a statement that characterizes the state of motion or equilibrium of the body, which may be based on energy principles and leads to equations referred to as balance equations, often expressed in terms of quantities called stress measures; (3) a constitutive law that accounts for the body material behavior. Such ingredients are introduced here along with a physical–mathematical model of the considered body.

Let us schematize a non-prismatic slender elastic body as a set of deformable plane figures (beam cross-sections) attached at a deformable line (beam center-line), occupying a spatial region of volume V in its undeformed reference state (Figure 1). The slenderness of the body is associated with a small value of the ratio h/L (i.e., $h/L \ll 1$), with h denoting the characteristic dimension or radius of the body cross-sections and L being the reference length of the body center-line. Let us consider a reference state of the body in which the cross-sections are orthogonal to the center-line at the centroid and the center-line is a straight regular curve. Moreover, the center-line may undergo large displacements, while the cross-sections follow the center-line motion and may undergo additional warping displacements, in and out of plane, which produce small cross-sectional deformations.

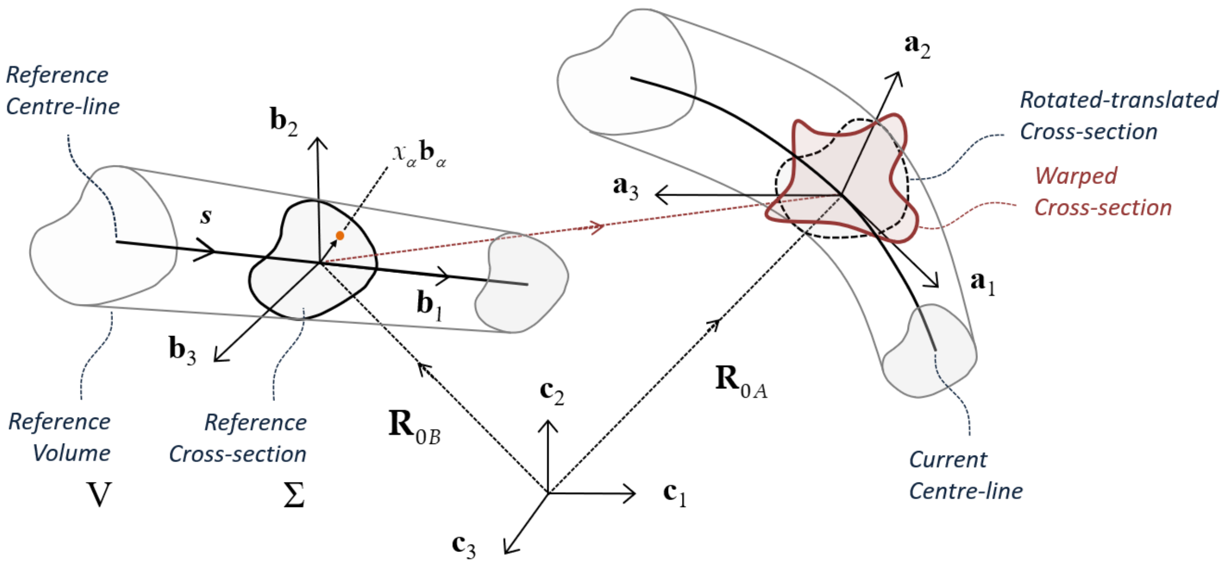

Figure 1. Schematic of a non-prismatic slender elastic body, occupying a region of volume V in its reference undeformed state (left), and a sketch of its current deformed state (right); the orange dot identifies a point in the reference undeformed cross-section (left); the deformed (warped) configuration of this latter is represented in red (right).

Figure 1 shows the reference and current states of center-line and cross-sections. Two local coordinate systems with orthogonal unit vectors are introduced. The first one, with unit vectors $\mathbf{b}_i$, i = 1, 2, 3, is defined at any point along the center-line in the reference state and depends on the arc-length s, i.e., $\mathbf{b}_i = \mathbf{b}_i(s)$. Note that $\mathbf{b}_1$ is tangential to the reference center-line, while $\mathbf{b}_2$ and $\mathbf{b}_3$ are contained in the cross-sectional plane. The second local coordinate system, with unit vectors $\mathbf{a}_i$, i = 1, 2, 3, is the image of the reference local coordinate system in the current state. It is called the current local coordinate system, and its position and orientation depend on the arc-length s and time t, i.e., $\mathbf{a}_i = \mathbf{a}_i(s,t)$. Note that unlike the reference (undeformed) state, in which a generic cross-section Σ is contained in the plane of $\mathbf{b}_2$ and $\mathbf{b}_3$, in the current (deformed) state a cross-section may not remain plane (un-warped) and may not belong to the plane of $\mathbf{a}_2$ and $\mathbf{a}_3$ because of the cross-sectional warping in and out of plane.

For convenience, we also introduce the orthogonal unit vectors $\mathbf{c}_1$, $\mathbf{c}_2$, and $\mathbf{c}_3$ associated with a fixed Cartesian reference frame (see Figure 1), and adopt a standard summation convention for indexed variables: Latin indices takes values 1, 2, and 3; Greek indices assume values 2 and 3; repeated indices are summed over their range.

The orientation of the local unit vectors $\mathbf{a}_i$ and $\mathbf{b}_i$ with respect to the fixed unit vectors $\mathbf{c}_i$ can be defined in terms of two proper orthogonal tensor fields, $\mathbf{A}$ and $\mathbf{B}$, such that the usual juxtaposition of these tensors to vectors of the fixed reference frame $\mathbf{c}_i$ provides vectors of the local coordinate systems, respectively, $\mathbf{a}_i = \mathbf{A}\mathbf{c}_i$, $\mathbf{b}_i = \mathbf{B}\mathbf{c}_i$, and i = 1, 2, 3.

Let us define the position of the beam points in the reference and current states via two mapping functions, $\mathbf{R}_B$ and $\mathbf{R}_A$, as follows:

$$\mathbf{R}_B(z_i) = \mathbf{R}_{0B}(z_1) + x_\alpha(z_i)\mathbf{b}_\alpha(z_1)\,, \tag{1a}$$

$$\mathbf{R}_A(z_i,t) = \mathbf{R}_{0A}(z_1,t) + x_\alpha(z_i)\mathbf{a}_\alpha(z_1,t) + w_k(z_i,t)\mathbf{a}_k(z_1,t)\,, \tag{1b}$$

where $\mathbf{R}_{0B}$ and $\mathbf{R}_{0A}$ denote the position of the center-lines in the reference and current states with respect to the fixed Cartesian reference system; x_α identify the points in the body cross-sections; w_i are warping displacements; and, finally, z_i are time-independent variables, with $z_1 = s$ and z_α spanning a two-dimensional domain such that $x_i = \Lambda_{ij}z_j$, with $\Lambda_{11} = 1$, $\Lambda_{22} = \Lambda_2(z_1)$, $\Lambda_{33} = \Lambda_3(z_1)$, and $\Lambda_{ij} = 0$ for $i \neq j$. Henceforth, the dependence of all scalar, vector, and tensor fields on the spatial variables z_i (or x_i) and on the time t is understood and, hence, omitted.

Let us describe the body state of strain via the Green–Lagrange strain tensor $\mathbf{E}$ and the vector fields $\boldsymbol{\gamma} = \mathbf{T}^T\mathbf{R}'_{0A} - \mathbf{R}'_{0B}$ and $\mathbf{k} = \mathbf{T}^T\mathbf{k}'_A - \mathbf{k}'_B$, as in [37], where $\mathbf{k}_B$ and $\mathbf{k}_A$ are axial vectors of the skew tensors $\mathbf{K}_B = \mathbf{B}'\mathbf{B}^T$ and $\mathbf{K}_A = \mathbf{A}'\mathbf{A}^T$, respectively; $\mathbf{T} = \mathbf{a}_i \otimes \mathbf{b}_i$, $\otimes$ is the usual dyadic product; and prime stands for s-derivative. Note that $\mathbf{k} = k_i\mathbf{b}_i$ and $\boldsymbol{\gamma} = \gamma_i\mathbf{b}_i$ (one-dimensional strain measures) describe variations in beam curvature and center-line tangent between the current and reference states, while $\mathbf{E} = E_{ij}\mathbf{b}_i \otimes \mathbf{b}_j$ (three-dimensional strain measure) accounts for the cross-sectional deformation and is defined as follows:

$$\mathbf{E} = \frac{\mathbf{H}^T\mathbf{H} - \mathbf{I}}{2}\,, \tag{2}$$

where $\mathbf{I}$ denotes the identity tensor, and $\mathbf{H}$ is the deformation gradient, i.e., the derivative of the current map $\mathbf{R}_A$ with respect to the reference map $\mathbf{R}_B$,

$$\mathbf{H} = \frac{\partial \mathbf{R}_A}{\partial \mathbf{R}_B}\,. \tag{3}$$

By combining (1)–(3), the components E_{ij} of the Green–Lagrange strain tensor (2) can be expressed in terms of one-dimensional strains (k_α, k_1, and γ_1, i.e., bending curvatures, torsional curvature, and center-line extension, respectively) and partial derivatives of the warping fields w_i. The dependence can be linear if such strain and warping fields are small, which is the case considered here. Specifically, we quantify this smallness by introducing a small dimensionless parameter $\varepsilon \ll 1$, representing the maximum among the orders of magnitude of the dimensionless quantities γ_i, hk_i, w_i/h, and $w_{i,j}$, and maintain only terms up to the first order in ε in the calculation of the scalar fields E_{ij} via Equation (2).

Let us describe the body state of stress via the second (symmetric) Piola–Kirchhoff stress tensor, $\mathbf{S} = S_{ij}\mathbf{b}_i \otimes \mathbf{b}_j$. Assuming small strains, as discussed in the foregoing, this stress tensor is related to the Green–Lagrange strain tensor via a linear elastic isotropic constitutive model [50], as follows:

$$\mathbf{S} = \frac{Y}{1+\nu}\mathbf{E} + \frac{\nu Y}{(1+\nu)(1-2\nu)}tr(\mathbf{E})\mathbf{I}\,, \tag{4}$$

where $tr(\mathbf{E}) = E_{ii}$, while Y (Young's modulus) and ν (Poisson's ratio) are material parameters. Stress tensors commonly used in mechanics are also the first Piola–Kirchhoff stress tensor $\mathbf{P} = \mathbf{HS}$ and the Cauchy stress tensor $\mathbf{C} = \mathbf{HSH}^T\det(\mathbf{H}^{-1})$, associated with the state of stress of the body in the current (deformed) configuration [50].

The stress and strain fields introduced so far can be obtained as solutions of balance equations, i.e., partial differential equations (PDEs) with the relevant boundary conditions, which are derivable via the principle of virtual power [16,51,52]. To exploit this principle, we define two functionals, namely, the external power $\boldsymbol{\Pi}_e$ and the internal power $\boldsymbol{\Pi}_i$. The external power functional $\mathbf{\Pi}_e$ is introduced to describe, for each velocity field attainable by the body, interactions between the body and the external environment. We imagine that such interactions may take place via contact and non-contact actions, and assume

$$\mathbf{\Pi}_e = \int_V \mathbf{f} \cdot \mathbf{v} + \int_{\partial V} \mathbf{p} \cdot \mathbf{v}\,, \tag{5}$$

where dot denotes the usual scalar or dot product in Euclidean vector space; vector $\mathbf{f}$ represents body loads (non-contact actions) per unit body reference volume V; vector $\mathbf{p}$ stands for surface loads (contact actions) per unit area of the body boundary ∂V; $\mathbf{v}$ is the time rate of the current position of the body points, i.e., the derivative of $\mathbf{R}_A$ with respect to time t; and, finally, the integrals are performed, respectively, over the body reference volume V (also represented in Figure 1, left) and its boundary ∂V. Interactions among the body parts are instead described via the internal power functional $\mathbf{\Pi}_i$, that is,

$$\mathbf{\Pi}_i = \frac{d}{dt} \int_V \Phi\,, \tag{6}$$

where $\Phi = \mathbf{S} \cdot \mathbf{E}/2$ is the body strain energy density, which can be explicitly expressed in terms of one-dimensional strains, k_α, k_1, γ_1, and cross-sectional warping fields w_i by using Equations (2)–(4). Balance equations are finally obtainable via the classical principle of virtual power, as in [16,28,45,51,52], by requiring that for any velocity field attainable by the body its interactions with the external environment and among its parts are such that the total power vanishes (i.e., $\mathbf{\Pi}_e = \mathbf{\Pi}_i$) at any value of the evolution parameter t.

Field Equations and Relevant PDE Problems

We are now in a position to introduce the field equations that govern the mechanical behavior of the considered elastic body. Following [28,45], for tapered straight beams, whose center-line and cross-sectional points are identified by the axial variable $s \in [0, L]$ and cross-sectional variables $(x_2, x_3) \in \Sigma$, the local coordinate system in the current state tangential to the deformed center-line, and external actions applied only at the end cross-sections (i.e., the cross-sections at $s = 0$ and $s = L$), the principle of virtual power allows us to write the following set of balance equations, i.e., partial differential equations,

$$\frac{\partial^2 \omega}{\partial x_2^2} + \frac{\partial^3 \omega}{\partial x_3^3} = 0\,, \tag{7a}$$

$$\frac{\partial \varphi_2}{\partial x_2} + \frac{\partial \varphi_3}{\partial x_3} = a_2 x_2 + a_3 x_3\,, \tag{7b}$$

$$\frac{\partial \varphi_3}{\partial x_2} - \frac{\partial \varphi_2}{\partial x_3} = b_2 x_2 + b_3 x_3\,, \tag{7c}$$

$$2(1-\nu)\frac{\partial^2 u_2}{\partial x_2^2} + (1-2\nu)\frac{\partial^2 u_2}{\partial x_3^2} + \frac{\partial^2 u_3}{\partial x_2 \partial x_3} + c_1 = 0\,, \tag{7d}$$

$$(1-2\nu)\frac{\partial^2 u_3}{\partial x_2^2} + 2(1-\nu)\frac{\partial^2 u_3}{\partial x_3^2} + \frac{\partial^2 u_2}{\partial x_3 \partial x_2} + d_1 = 0\,, \tag{7e}$$

with Neumann-type boundary conditions,

$$\left(\frac{\partial \omega}{\partial x_2} - k_1 x_3\right) n_2 + \left(\frac{\partial \omega}{\partial x_3} + k_1 x_2\right) n_3 = 0\,, \tag{8a}$$

$$\varphi_2 n_2 + \varphi_3 n_3 = 0\,, \tag{8b}$$

$$\left(2(1-\nu)\frac{\partial u_2}{\partial x_2} + 2\nu\frac{\partial u_3}{\partial x_3} + c_2\right) n_2 + (1-2\nu)\left(\frac{\partial u_2}{\partial x_3} + \frac{\partial u_3}{\partial x_2} + c_3\right) n_3 = 0\,, \tag{8c}$$

$$(1-2\nu)\left(\frac{\partial u_3}{\partial x_2}+\frac{\partial u_2}{\partial x_3}+d_2\right)n_2+\left(2(1-\nu)\frac{\partial u_3}{\partial x_3}+2\nu\frac{\partial u_2}{\partial x_2}+d_3\right)n_3=0\,. \tag{8d}$$

In (7) and (8), n_α represent the components of the outward unit normal on the boundary $\partial\Sigma$ of the cross-sectional domain Σ, while coefficients a_α, b_α, c_i, and d_i are defined as follows

$$a_2=2(1+\nu)k_3'+2(1+\nu)(\Lambda_3^{-1}\Lambda_3'+2\Lambda_2^{-1}\Lambda_2')k_3\,, \tag{9a}$$

$$a_3=-2(1+\nu)k_2'-2(1+\nu)(\Lambda_2^{-1}\Lambda_2'+2\Lambda_3^{-1}\Lambda_3')k_2\,, \tag{9b}$$

$$b_2=2\nu k_2'+2(1+\nu)\Lambda_2^{-1}\Lambda_2'k_2\,, \tag{9c}$$

$$b_3=2\nu k_3'+2(1+\nu)\Lambda_3^{-1}\Lambda_3'k_3\,, \tag{9d}$$

$$c_1=-(1-2\nu)k_1'x_3+\frac{\partial^2\omega}{\partial x_1\partial x_2}\,, \tag{9e}$$

$$c_2=2\nu\frac{\partial\omega}{\partial x_1}-(1-2\nu)\left(\frac{\partial\omega}{\partial x_2}-k_1x_3\right)\Lambda_2^{-1}\Lambda_2'x_2\,, \tag{9f}$$

$$c_3=-\left(\frac{\partial\omega}{\partial x_2}-k_1x_3\right)\Lambda_3^{-1}\Lambda_3'x_3\,, \tag{9g}$$

$$d_1=(1-2\nu)k_1'x_2+\frac{\partial^2\omega}{\partial x_1\partial x_3}\,, \tag{9h}$$

$$d_2=-\left(\frac{\partial\omega}{\partial x_3}+k_1x_2\right)\Lambda_2^{-1}\Lambda_2'x_2\,, \tag{9i}$$

$$d_3=2\nu\frac{\partial\omega}{\partial x_1}-(1-2\nu)\left(\frac{\partial\omega}{\partial x_3}+k_1x_2\right)\Lambda_3^{-1}\Lambda_3'x_3\,. \tag{9j}$$

The unknown scalar fields ω, φ_2, φ_3, u_2, u_3, depending on variables x_i, can be determined as functions of taper coefficients Λ_α and one-dimensional strains, γ_1 and k_i, by solving the PDE problems (7)–(9). In its turn, given the scalar fields ω, φ_2, φ_3, u_2, u_3, introduced to formulate the PDE problems (7)–(9) in a more compact form, the components E_{ij} of the Green–Lagrange strain tensor can be determined via the following relations:

$$E_{11}=\frac{\partial\omega}{\partial x_1}+\gamma_1+k_2x_3-k_3x_2\,, \tag{10a}$$

$$2E_{12}=\frac{\partial\omega}{\partial x_2}+\varphi_2-k_1x_3+2(1+\nu)(\gamma_1+k_2x_3-k_3x_2)\Lambda_2^{-1}\Lambda_2'x_2\,, \tag{10b}$$

$$2E_{13}=\frac{\partial\omega}{\partial x_3}+\varphi_3+k_1x_2+2(1+\nu)(\gamma_1+k_2x_3-k_3x_2)\Lambda_3^{-1}\Lambda_3'x_3\,, \tag{10c}$$

$$E_{22}=\frac{\partial u_2}{\partial x_2}-\nu(\gamma_1+k_2x_3-k_3x_2)\,, \tag{10d}$$

$$E_{33}=\frac{\partial u_3}{\partial x_3}-\nu(\gamma_1+k_2x_3-k_3x_2)\,, \tag{10e}$$

$$2E_{23}=\frac{\partial u_2}{\partial x_3}+\frac{\partial u_3}{\partial x_2}\,. \tag{10f}$$

Equations (7)–(10) show the role, from a mechanical standpoint, played by the scalar fields ω, φ_2, φ_3, u_2, and u_3, in the determination of the strain fields E_{ij}. Specifically, ω, φ_2, and φ_3 affect the Green–Lagrange strains E_{11}, E_{21}, and E_{31} associated with the out-of-plane deformation of the body cross-sections, while the scalar fields u_2 and u_3 affect only the Green–Lagrange strains E_{22}, E_{33}, and E_{23} associated with the in-plane deformations. In particular, the scalar field ω plays the role of the de Saint-Venant's out-of-plane warping function, to which it is proportional via the torsional curvature k_1. Moreover, its determination does not depend on the determination of the other scalar fields, i.e., the PDE (7a) with boundary condition (8a) is an independent PDE problem. Similarly, the PDEs (7b) and (7c) with boundary condition (8b) and the PDEs (7d) and (7e) with boundary conditions (8c) and (8d) are two PDE problems that can be solved independently of each other: the first problem is in terms of the scalar fields φ_2, φ_3, which are a measure of the cross-sectional shear strains produced by the body flexure; the second problem is in terms of the scalar fields u_2 and u_3, which govern the in-plane deformation of the body cross-sections. We also note that all PDE problems formally resemble those that govern the deformation of the de Saint-Venant's cylinder [7,8], except for the coefficients a_α, b_α, c_i, and d_i, which in the present work account for the effects of taper and reduce to those of the de Saint-Venant's cylinder only in the prismatic case. Finally, it is worth noting that the solution of the PDE problems (7)–(9) and, as a consequence, the components of the Green–Lagrange strain tensor (10) explicitly depend on the taper functions Λ_α and can be expressed in terms of linear combinations of the one-dimensional strains, γ_1 and k_i, and their s-derivative. This allows us to consider separately the effect of each one-dimensional strain measure by solving simpler PDE problems whose solutions only depend on the shape of the cross-sectional domain Σ. Unfortunately, even such simpler problems, which can always be solved numerically, admit closed-form analytical solutions only in a few cases (see, e.g., Section 3). However, apart from determining the scalar fields ω, φ_2, φ_3, u_2, and u_3, and the corresponding strain fields (10) and stress fields (4), it is also possible to obtain analytical solutions in terms of other mechanical quantities of interest for engineering applications, as discussed in Section 4.

3. Analytical Solution in the Case of Circular Cross-Sections

As anticipated in the foregoing, the PDE problem (7)–(9) admits closed-form analytical solutions only in a few cases. This is the case, for instance, of tapered beams with circular cross-sections of radius $R(s)$ and taper functions $\Lambda_2 = \Lambda_3 = \Lambda(s)$, subject to bending and extension (and null torsional curvature k_1). In such case, the identically null scalar field ω satisfies PDE problem (7a), (8a), as do null scalar fields u_2 and u_3 with PDE problem (7b), (7c), and (8b). On the contrary, the scalar fields φ_2 and φ_3 depend on bending curvatures k_α and center-line extension γ_1, which are not null in the present case. However, for the cross-sectional shape considered in this section, it is possible to find closed-form expressions of φ_2 and φ_3 that satisfy the PDE problem (7d), (7e), (8c), and (8d). They are

$$\varphi_2 = \left(\frac{1-2\nu}{4}x_3^2 + \frac{3+2\nu}{4}(x_2^2 - R^2)\right)k_3' - \frac{1+2\nu}{2}x_2x_3k_2' + 2(1+\nu)\Lambda^{-1}\Lambda'\left((x_2^2 - R^2)k_3 - x_2x_3k_2\right), \tag{11a}$$

$$\varphi_3 = -\left(\frac{1-2\nu}{4}x_2^2 + \frac{3+2\nu}{4}(x_3^2 - R^2)\right)k_2' + \frac{1+2\nu}{2}x_2x_3k_3' - 2(1+\nu)\Lambda^{-1}\Lambda'\left((x_3^2 - R^2)k_2 - x_2x_3k_3\right). \tag{11b}$$

Given the scalar fields ω, φ_2, φ_3, u_2, and u_3, it is possible to determine the components of the Green–Lagrange strain tensor (10) and, subsequently, by using the constitutive model, the corresponding stress fields (4). By combining (11) and (10), the following expressions are obtained for the components of the Green–Lagrange strain tensor

$$E_{11} = \gamma_1 + k_2x_3 - k_3x_2\,, \tag{12a}$$

$$2E_{12} = \left(\frac{1-2\nu}{4}x_3^2 + \frac{3+2\nu}{4}(x_2^2 - R^2)\right)k_3' - \frac{1+2\nu}{2}x_2x_3k_2' + 2(1+\nu)\Lambda^{-1}\Lambda'\left(x_2\gamma_1 - R^2k_3\right), \tag{12b}$$

$$2E_{13} = -\left(\frac{1-2\nu}{4}x_2^2 + \frac{3+2\nu}{4}(x_3^2 - R^2)\right)k_2' + \frac{1+2\nu}{2}x_2x_3k_3' + 2(1+\nu)\Lambda^{-1}\Lambda'\left(x_3\gamma_1 + R^2k_2\right), \tag{12c}$$

$$E_{22} = -\nu(\gamma_1 + k_2x_3 - k_3x_2), \tag{12d}$$

$$E_{33} = -\nu(\gamma_1 + k_2x_3 - k_3x_2), \tag{12e}$$

$$2E_{23} = 0. \tag{12f}$$

Equation (12) formally resembles those valid for a prismatic cylinder with circular cross-sections [7], except for the additional terms depending on the taper function $\Lambda(s)$ and for the dependence of the cross-sectional radius $R(s)$ on the arc-length s.

The above solution provides an analytical demonstration of the inadequacy of a stepped beam approach when dealing with predictions of stresses and strains in tapered beams. As is apparent, it is not possible to account for all the effects of taper only by taking the formal solutions of the prismatic beam theory and considering the variation of the cross-section geometric parameters with s (e.g., $R(s)$): the additional non-trivial terms depending on taper functions (e.g., $\Lambda(s)$), which are present in the expressions of the stress and strain fields in tapered elements, cannot be taken into account with such an approach.

4. Analytical Solution in Terms of Cross-Sectional Strain Flow

Let us consider a simply connected two-dimensional domain Σ_q contained in the cross-sectional domain Σ, as in Figure 2, where the cross-sectional domain Σ is split in two zones: the dashed one coincides with the domain Σ_q. The boundary of this latter, whose normal and tangent vectors are denoted as $\mathbf{n}$ and $\mathbf{t}$, is oriented counterclockwise and is composed by several lines: a line fully contained in the interior of the cross-sectional domain Σ is referred to as an internal line, $\partial\Sigma_i$; a line that coincides with a part of the boundary of the cross-sectional domain Σ is an external line, $\partial\Sigma_e$. For completeness, we also define the components n_α and t_α of the normal and tangent vectors $\mathbf{n}$ and $\mathbf{t}$, respectively.

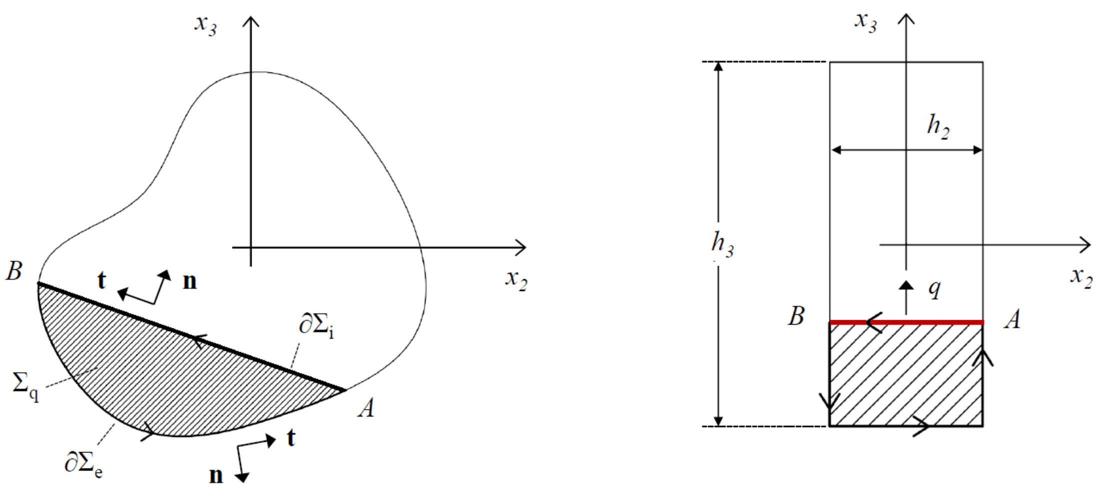

Figure 2. Schematic of a generic cross-section with indication of the two-dimensional domain Σ_q and its boundary lines, $\partial\Sigma_i$ and $\partial\Sigma_e$ (left), and case of the rectangular cross-section (right).

Let us introduce the cross-sectional strain flow q as a measure of the flow of the strain fields $E_{1\alpha}$ through the boundary lines $\partial\Sigma_i$. It is defined via the line integral

$$q = \int_{\partial\Sigma_i} 2E_{1\alpha}n_\alpha \,. \tag{13}$$

The strain flow q is a mechanical quantity of interest in engineering applications and provides a measure of the mean shear strain in the interior of the body cross-sections. To actually determine the strain flow q, we have to calculate the line integral (13). To this aim, we can exploit Green's formulas or the divergence theorem [50]. In fact, according to the divergence theorem, the line integral of the flow of strain fields $E_{1\alpha}$ over the boundary of a two-dimensional domain Σ_q coincides with the surface integral of the divergence of the same strain fields $E_{1\alpha}$ over the domain Σ_q. In its turn, the divergence of $E_{1\alpha}$ is expressible in terms of divergence of the scalar fields φ_α, appearing in Equations (7)–(10). Following the procedure illustrated now, which begins from definition (13), exploitation of Equations (7)–(10), and integration based on Green's formulas or on the divergence theorem, after some algebraic manipulation, the strain flow q can be expressed in the form

$$\frac{q}{2(1+\nu)} = -S_2k_2' + S_3k_3' - Z_2k_2 + Z_3k_3 + Z_1\gamma_1 \,, \tag{14}$$

where coefficients S_α are the static moments of the two-dimensional domain Σ_q with respect to the cross-sectional axes x_α and are defined via the surface integrals

$$S_2 = \int_{\Sigma_q} x_3 \,, S_3 = \int_{\Sigma_q} x_2 \,, \tag{15}$$

while Z_i are geometric coefficients that explicitly depend on taper functions and are defined via line integrals over the internal boundary $\partial\Sigma_i$ of the domain Σ_q as follows:

$$Z_1 = \Lambda_2^{-1}\Lambda_2' \int_{\partial\Sigma_i} x_2n_2 + \Lambda_3^{-1}\Lambda_3' \int_{\partial\Sigma_i} x_3n_3 \,, \tag{16a}$$

$$Z_2 = S_2' + \Lambda_2^{-1}\Lambda_2' \int_{\partial\Sigma_i} x_3x_2n_2 + \Lambda_3^{-1}\Lambda_3' \int_{\partial\Sigma_i} x_3x_3n_3 \,, \tag{16b}$$

$$Z_3 = S_3' + \Lambda_2^{-1}\Lambda_2' \int_{\partial\Sigma_i} x_2x_2n_2 + \Lambda_3^{-1}\Lambda_3' \int_{\partial\Sigma_i} x_2x_3n_3 \,, \tag{16c}$$

Equations (14)–(16) show the analytical dependence of the cross-sectional strain flow q on the one-dimensional strains (bending curvatures k_α and center-line extension γ_1) and on the cross-sectional taper (via the taper functions Λ_α). It is worth noting that in the prismatic case, coefficients Z_i identically vanish and the cross-sectional strain flow q turns out to be a linear combination of the s-derivative of the bending curvatures k_α, the coefficients of the linear combination being the static moments S_α, as is expected from the classical linear theory of prismatic beams [7,8].

Application Example

Equation (14) can provide application-oriented information. As an example, let us consider a structural element widely employed in applications, i.e., a tapered beam with rectangular cross-sections. See Figure 2 (right): the cross-sectional axes x_2 and x_3 are parallel to the edges of length h_2 and h_3, respectively; the relevant taper functions are Λ_2 and Λ_3. Within this cross-section, let us consider a cross-sectional chord (AB) parallel to the x_2-axis. The strain flow through such chord can be obtained using Equations (14)–(16) and performing all surface and line integrals. The following result is obtained

$$\frac{q}{(1+\nu)h_2} = -\Lambda_2^{-1}(\Lambda_2k_2)'\frac{4x_3^2 - h_3^2}{4} + \Lambda_3^{-1}\Lambda_3'\frac{h_3^2k_2 + 4x_3\gamma_1}{2} \,, \tag{17}$$

where x_α and h_α are cross-sectional variables and dimensions of the cross-section at the axial coordinate s; k_2 and γ_1 are bending curvature and center-line extension; and, finally, the effects of taper are accounted for by taper functions Λ_α.

This paradigmatic example shows the influence of cross-sectional taper on the strain flow q and a typical cross-sectional distribution of this latter in tapered elements, which (for rectangular cross-sections) is quadratic with respect to the cross-sectional variable x_3 when it is evaluated on cross-sectional chords parallel to the x_2-axis. It is evident that the strain flow depends not only on the cross-sectional variable x_3 but also on the axial variable s, i.e., the strain flow distribution is different on different cross-sections: Equation (17) provides a quantitative measure of this dependence, which vanishes in the prismatic case, as is expected. Moreover, we also observe, once again, the inadequacy of stepped-beam approaches when dealing with predictions of stresses and strains in non-prismatic elements: with regard to the present example, the additional terms depending on the cross-sectional taper (e.g., taper functions Λ_α in Equation (17)) cannot be accounted for by a stepped-beam approach. The usefulness of analytical solutions such as those discussed in this work is evident: they allow analytical predictions (about the influence of taper, for instance) to be performed in a straightforward manner and provide an insight into the physical problem which is not achievable via purely numerical investigations.

5. Conclusions

Slender elastic solids with non-prismatic cross-sections are prototypical models of many structural elements used in engineering applications. An accurate analytical prediction of their state of stress and strain is much more complex than in prismatic elements because of the additional non-trivial stress and strain fields produced by the cross-sectional taper that are absent in prismatic elements and that cannot be predicted by exploiting the results available for these latter, as demonstrated in the paper.

Specifically, this work has addressed the physical–mathematical modeling and the analytical prediction of cross-sectional strains and stresses, in and out of plane, in non-prismatic slender solids susceptible to large deflections. A variational principle has provided the field equations, i.e., the set of partial differential equations (PDEs) and boundary conditions that govern the state of stress and strain in the considered elastic solids. The obtained equations represent a generalization of those that govern the state of deformation of the classical de Saint-Venant's cylinder and reduce exactly to them for a prismatic cylinder undergoing small displacements and strains.

Two analytical solutions to the aforementioned PDEs are discussed: the first is valid for circular cross-sectioned tapered beams undergoing bending and extension. For this case, analytical closed-form expressions can be obtained for the in- and out-of-plane cross-sectional strains and the corresponding stress fields. The second solution is valid for slender elastic solids with generic tapered cross-sections. For such solids, a closed-form solution in terms of cross-sectional strain flow has been obtained. An application example is also reported to show how such a closed-form expression of the strain flow can be used to derive application-oriented information.

The analytical results reported and discussed in the paper have regarded the strain and stress fields in tapered slender solids and the effects of taper. Analytical investigations generally provide an insight into physical problems not achievable via purely numerical analyses and, in the present work, have also provided an analytical demonstration of the inadequacy of stepped-beam approaches when dealing with predictions of stresses and strains in tapered slender solids. Apart from the effects of taper, analytical investigations regarding the influence of other geometric parameters (e.g., cross-sectional pre-twist and center-line initial curvature) and material properties (inhomogeneity and anisotropy) on cross-sectional strains, both in and out of plane, as well as on other mechanical quantities (e.g., strain flow), would be important and will be addressed in subsequent works.

Funding: This research received no external funding.

Data Availability Statement: Data are contained within the article.

Conflicts of Interest: The author declares no conflict of interest.

References

1. Atkin, E. Tapered Beams: Suggested Solutions for Some Typical Aircraft Cases. *Aircr. Eng. Aerosp. Technol.* **1938**, *10*, 347–351. [CrossRef]
2. Buckney, N.; Green, S.; Pirrera, A.; Weaver, P.M. On the structural topology of wind turbine blades. *Thin-Walled Struct.* **2013**, *67*, 144–154. [CrossRef]
3. Griffith, D.T.; Ashwill, T.D.; Resor, B.R. Large offshore rotor development: Design and analysis of the Sandia 100-meter wind turbine blade. In Proceedings of the 53rd Structures, Structural Dynamics and Materials Conference, Honolulu, HI, USA, 23–26 April 2012.
4. Migliaccio, G. Analytical determination of the influence of geometric and material design parameters on the stress and strain fields in non-prismatic components of wind turbines. *J. Phys. Conf. Ser.* **2022**, *2265*, 032033. [CrossRef]
5. Paglietti, A.; Carta, G. Remarks on the current theory of shear strength of variable depth beams. *Open Civ. Eng. J.* **2009**, *3*, 28–33. [CrossRef]
6. Love, A. *A Treatise on the Mathematical Theory of Elasticity*; Dover Publications: New York, NY, USA, 1944.
7. Sokolnikoff, I. *Mathematical Theory of Elasticity*; McGraw-Hill Inc.: New York, NY, USA, 1946.
8. Muskhelishvili, N. *Some Basic Problems of the Mathematical Theory of Elasticity*; Springer: Dordrecht, The Netherlands, 1977.
9. Simo, J. A finite strain beam formulation, the three-dimensional dynamic problem, part I. *Comput. Methods Appl. Mech. Eng.* **1985**, *49*, 55–70. [CrossRef]
10. Reissner, E. On one-dimensional large-displacement finite-strain beam theory. *Stud. Appl. Math.* **1973**, *2*, 87–95. [CrossRef]
11. Reissner, E. On finite deformation of space curved beams. *J. Appl. Math. Phys.* **1981**, *32*, 734–744. [CrossRef]
12. Antman, S.; Warner, W. Dynamical theory of hyper-elastic rods. *Arch. Rational Mech. Anal.* **1966**, *23*, 135–162. [CrossRef]
13. Ibrahimbegovic, A. On finite element implementation of geometrically nonlinear Reissner's beam theory: Three-dimensional curved beam elements. *Comput. Methods Appl. Mech. Eng.* **1995**, *122*, 11–26. [CrossRef]
14. Simo, J. A three-dimensional finite-strain rod model, part II: Computational aspects. *Comput. Methods Appl. Mech. Eng.* **1986**, *58*, 79–116. [CrossRef]
15. Cosserat, E.; Cosserat, F. *Théorie des Corps Déformables*; A. Hermann et Fils: Paris, France, 1909.
16. Rubin, M. *Cosserat Theories: Shells, Rods and Points. Solid Mechanics and Its Applications*; Kluwer Academic Publishers: Dordrecht, The Netherlands, 2000; Volume 79.
17. Berdichevsky, V. On the theory of curvilinear Timoshenko-type rods. *Prikl. Matem. Mekhan.* **1983**, *47*, 1015–1024. [CrossRef]
18. Yu, W.; Hodges, D.; Ho, J. Variational asymptotic beam-sectional analysis—An updated version. *Int. J. Eng. Sci.* **2012**, *59*, 40–64. [CrossRef]
19. Hodges, D.H.; Rajagopal, A.; Ho, J.C.; Yu, W. Stress and strain recovery for the in-plane deformation of an isotropic tapered strip-beam. *J. Mech. Mater. Struct.* **2010**, *5*, 963–975. [CrossRef]
20. Carrera, E.; Pagani, A. Unified formulation of geometrically nonlinear refined beam theories. *Mech. Adv. Mater. Struct.* **2016**, *25*, 15–31.
21. Ghayesh, M. Nonlinear vibration analysis of axially functionally graded shear-deformable tapered beams. *Appl. Math. Model.* **2018**, *59*, 583–596. [CrossRef]
22. Carrera, E.; Pagani, A.; Petrolo, M.; Zappino, E. Recent developments on refined theories for beams with applications. *Mech. Eng. Rev.* **2015**, *2*, 298–311. [CrossRef]
23. Goodier, G.; Griffin, D. Elastic bending of pretwisted bars. *Int. J. Solids Struct.* **1969**, *5*, 1231–1245. [CrossRef]
24. Rosen, A. The effect of initial twist on the torsional rigidity of beams—Another point of view. *J. Appl. Mech.* **1980**, *47*, 389–392. [CrossRef]
25. Hodges, D. Torsion of pretwisted beams due to axial loading. *J. Appl. Mech.* **1980**, *47*, 393–397. [CrossRef]
26. Krenk, S. The torsion-extension coupling in pretwisted elastic beams. *Int. J. Solids Struct.* **1983**, *19*, 67–72. [CrossRef]
27. Rosen, A. Theoretical and experimental investigation of the nonlinear torsion and extension of initially twisted bars. *J. Appl. Mech.* **1983**, *50*, 321–326. [CrossRef]
28. Migliaccio, G.; Ruta, G. The influence of an initial twisting on tapered beams undergoing large displacements. *Meccanica* **2021**, *56*, 1831–1845. [CrossRef]
29. Balduzzi, G.; Hochreiner, G.; Füssl, J. Stress recovery from one dimensional models for tapered bi-symmetric thin-walled I beams: Deficiencies in modern engineering tools and procedures. *Thin-Walled Struct.* **2017**, *119*, 934–945. [CrossRef]
30. Migliaccio, G. Non-prismatic beamlike structures with 3D cross-sectional warping. In Proceedings of the 14th World Congress in Computational Mechanics (WCCM) and ECCOMAS Congress 2020, Paris, France, 11–15 January 2021.
31. Migliaccio, G.; Ruta, G.; Barsotti, R.; Bennati, S. A new shear formula for tapered beamlike solids undergoing large displacements. *Meccanica* **2022**, *57*, 1713–1734. [CrossRef]

32. Slocum, S. A general formula for the shearing deflection of arbitrary cross-section, either variable or constant. *J. Frankl. Inst.* **1911**, *171*, 365–389. [CrossRef]
33. Krahula, J. Shear formula for beams of variable cross section. *AIAA J.* **1975**, *13*, 1390–1391. [CrossRef]
34. Xu, Y.; Zhou, D. Elasticity solution of multi-span beams with variable thickness under static loads. *Appl. Math. Model.* **2009**, *33*, 2951–2966. [CrossRef]
35. Mercuri, V.; Balduzzi, G.; Asprone, D.; Auricchio, F. Structural analysis of non-prismatic beams: Critical issues, accurate stress recovery, and analytical definition of the finite element (FE) stiffness matrix. *Eng. Struct.* **2020**, *213*, 110252. [CrossRef]
36. Lee, J.; Lee, J. An exact transfer matrix expression for bending vibration analysis of a rotating tapered beam. *Appl. Math. Model.* **2018**, *53*, 167–188. [CrossRef]
37. Migliaccio, G.; Ruta, G. Rotor blades as curved, twisted, and tapered beam-like structures subjected to large deflections. *Eng. Struct.* **2020**, *222*, 111089. [CrossRef]
38. Bertolini, P.; Eder, M.A.; Taglialegne, L.; Valvo, P.S. Stresses in constant tapered beams with thin-walled rectangular and circular cross sections. *Thin-Walled Struct.* **2019**, *137*, 527–540. [CrossRef]
39. Navier, C. *Résumé des Leçons Données à L'école des Ponts et Chaussées sur l'Application de la Mécanique a L'établissement des Constructions et des Machines*, 3rd ed.; avec des notes étendues par M. Barré de Saint-Venant; Dunod: Paris, France, 1864.
40. Jourawski, D. Sur la résistance d'un corps prismatique et d'une piéce composée en bois ou on tôle de fer à une force perpendiculaire à leur longeur. *Ann. Ponts Chaussées* **1856**, *12*, 328–351.
41. Bleich, F. *Stahlhochbauten Bd. 1*; Springer: Berlin, Germany, 1932.
42. Balduzzi, G.; Aminbaghai, M.; Sacco, E.; Füssl, J.; Eberhardsteiner, J.; Auricchio, F. Non-prismatic beams: A simple and effective Timoshenko-like model. *Int. J. Solid Struct.* **2016**, *90*, 236–250. [CrossRef]
43. Pugsley, A.; Weatherhead, R. The Shear Stresses in Tapered Beams. *Aeronaut. J.* **1942**, *46*, 218–226. [CrossRef]
44. Saksena, G. Shear Stress in a Tapering Beam. *Aircr. Eng. Aerosp. Technol.* **1944**, *16*, 47–50. [CrossRef]
45. Migliaccio, G. Analytical evaluation of stresses and strains in inhomogeneous non-prismatic beams undergoing large deflections. *Acta Mech.* **2022**, *233*, 2815–2827. [CrossRef]
46. Migliaccio, G. Analytical prediction of the cross-sectional shear flow in non-prismatic inhomogeneous beamlike solids. *Thin-Walled Struct.* **2023**, *183*, 110384. [CrossRef]
47. Matevossian, H. Asymptotics and uniqueness of solutions of the elasticity system with the mixed Dirichlet-Robin boundary conditions. *Mathematics* **2020**, *8*, 2241. [CrossRef]
48. Matevossian, H.A.; Nikabadze, M.U.; Nordo, G.; Ulukhanyan, A.R. Biharmonic Navier and Neumann problems and their application in mechanical engineering. *Lobachevskii J. Math.* **2021**, *42*, 1876–1885. [CrossRef]
49. Matevossian, H. Dirichlet-Neumann problem for the biharmonic equation in exterior domains. *Differ. Equ.* **2021**, *57*, 1020–1033. [CrossRef]
50. Gurtin, M. *An Introduction to Continuum Mechanics, Mathematics in Science and Engineering*; Academic Press: Pittsburgh, PA, USA, 1981.
51. Dell'Isola, F.; Bichara, A. *Elementi di Algebra Tensoriale con Applicazioni alla Meccanica dei Solidi*; Società Editrice Esculapio: Bologna, Italy, 2005.
52. Ruta, G.; Pignataro, M.; Rizzi, N. A direct one-dimensional beam model for the flexural-torsional buckling of thin-walled beams. *J. Mech. Mater. Struct.* **2006**, *1*, 1479–1496. [CrossRef]